Scanning Tunneling Microscopy and Surface Simulation of Zinc-Blende GaN(001) Intrinsic 4× Reconstruction: Linear Gallium Tetramers?

Hamad A. H. AL-Brithen, Rong Yang, Muhammad B. Haider, Costel Constantin, Erdong Lu, and Arthur R. Smith

Condensed Matter and Surface Science Program, Department of Physics and Astronomy, Ohio University, Athens, Ohio 45701, USA

Nancy Sandler and Pablo Ordejón

Condensed Matter and Surface Science Program, Department of Physics and Astronomy, Ohio University, Athens, Ohio 45701, USA
Instituto de Ciencia de Materiales de Barcelona–CSIC, Campus UAB, 08193 Bellaterra, Barcelona, Spain

(Received 22 August 2004; published 28 September 2005)

Scanning tunneling microscopy images confirm electron difraction studies that the zinc-blende GaN(001)-4× reconstruction consists of rows aligned along [110] with a spacing along $[1\bar{1}0]$ of $4a$. Dual-bias imaging shows a 180° shift of the corrugation maximum position between the profiles of empty and occupied states, in agreement with surface simulations based on the 4×1 linear tetramer model of Neugebauer *et al.* [Phys. Rev. Lett. **80**, 3097 (1998)]. Electronic structure calculations predict a surface band gap of 1.1 eV, close to the measured value of 1.14 eV and the previously predicted value (1.2 eV). Despite the successes of this model, high-resolution images reveal an unexpected 3× periodicity (not seen in diffraction) along the [110] row direction, indicating the need for a 4×3 model, and putting into question the existence of linear Ga tetramers.

DOI: 10.1103/PhysRevLett.95.146102 PACS numbers: 68.35.Bs, 68.37.Ef, 73.20.At

Based on both fundamental and technological motivations, reconstructions occurring on almost every metal, semiconductor, superconductor, and even certain oxide, surfaces have been investigated and imaged directly with scanning tunneling microscopy (STM) [1–3]. In particular, reconstructions of the (001) surfaces of III-V semiconductors have been explored intensively for the past 30 years [4,5]. Many of these surfaces lower energy through the formation of dimers [6–8]. Interestingly, MacPherson *et al.* reported STM images of InP(001)-(2×4), finding evidence for an unusual ''trimerlike'' structure [9]. The question then arises: does any III-V (001) semiconductor surface have a ''tetramer'' reconstruction?

GaN surfaces exhibit a variety of novel reconstructions that are not found on more conventional III-V surfaces [10,11]. An example is the intrinsic reconstruction of wurtzite GaN$(000\bar{1})$, which was found to be a monolayer of Ga atoms atop the N-terminated bilayer [10]. No such structure is found on GaAs, for example, since the Ga-Ga distance (4.00 Å) would be much larger than in bulk Ga metal (2.7 Å), rendering the monolayer unstable. As another example, the stable GaN(0001) surface consists of a double Ga layer, which is crucial for the growth of atomically smooth GaN surfaces.

Reconstructions on zinc-blende (c-)GaN(001) were reported by several groups using STM and reflection high energy electron diffraction (RHEED), including 1×1, 2×2, $c(2 \times 2)$, and $\sqrt{10} \times \sqrt{10}$-R18.4° [12,13]. However, several of these structures were later reproduced by exposing the clean surface during growth to an arsenic background, whereas, without the As, only 1×1 and 4×1 were observed in diffraction [14]. Theoretical insight into the intrinsic surface reconstructions of c-GaN(001) followed shortly thereafter, first by Neugebauer *et al.* and then by others [15,16], who predicted that the intrinsic structure is 4×1 consisting of a novel linear Ga tetramer unit. The 4×1 tetramer model exactly satisfies electron counting, whereas 4×1 trimer, dimer, and monomer models do not. However, this unusual reconstruction has not up to now been observed using STM.

In this Letter, we present STM data of the c-GaN(001) surface, in which both filled and empty components of the native 4× surface reconstruction are shown. In addition, the local density of states is probed by scanning tunneling spectroscopy (STS). We also present *ab initio* calculations (using the SIESTA method) and STM simulations for the tetramer model of Neugebauer *et al.* We consider the degree of agreement of the experimental data with the 4×1 tetramer model.

Cubic GaN layers are grown by rf N-plasma molecular beam epitaxy (MBE) on MgO(001) with an effusion cell for gallium. Prior to GaN growth, the MgO(001) substrate is heated to 900–1000 °C (measured by an optical pyrometer with emissivity set at 0.7) with the nitrogen plasma turned on for ~30 min. Then, GaN growth takes place with the substrate temperature (T_S) set at ~580 °C and the base pressure of nitrogen and the plasma source power set at 9×10^{-6} Torr and 500 W, respectively.

The growth, under Ga-rich conditions (Ga flux $\sim 2.3 \times 10^{14}/\mathrm{cm}^2$ sec) is monitored using RHEED. The film corresponding to the 4× STM images shown here was ~3800 Å thick. The *in-plane* and *out-of-plane* lattice constants were each separately measured to be 4.53 Å, in excellent agreement with the reported strain-relaxed value of 4.52 ± 0.05 Å [17]. The MBE-grown sample (with or without annealing) is transferred directly to the adjoining

STM chamber under ultrahigh vacuum. The *in situ* STM and STS measurements are performed at 300 K.

Figure 1(a) shows a RHEED pattern of the surface at $T_S = 490\,^{\circ}\mathrm{C}$ after growth; similar patterns are observed during growth. The cubic phase identity and crystalline film orientation have been verified using cathodoluminescence (CL), optical absorption, atomic force microscopy, and x-ray diffraction [18]. The epitaxial orientation has been found to be $\langle 001\rangle_{c\text{-GaN}} \| \langle 001\rangle_{\mathrm{MgO}}$ and $\langle 110\rangle_{c\text{-GaN}} \| \langle 110\rangle_{\mathrm{MgO}}$.

Cubic GaN(001) grown under Ga-rich conditions exhibits 1×1 RHEED at high temperatures; but as seen in Fig. 1(b), after cooling to 300 K, $2\times$ and even weak $8\times$ streaks are observed. In Fig. 1(c), the corresponding STM image of the as-grown surface reveals a row reconstruction with row spacing of $8a$ where a (the nearest neighbor Ga-Ga spacing) $= a_{\text{conventional cell}}/\sqrt{2}$. Each row consists of rectangular-shaped units spaced apart by $2a$, which alternate with 2 characteristic lengths. Since this $c(4 \times 16)$ reconstruction forms only after cooling and is removed by annealing, it is evidently composed of Ga adatoms atop the Ga-terminated GaN(001). Several other adatom reconstructions are also found on the Ga-rich surface, including 4×7 and $c(4 \times 20)$.

After annealing the surface at $T_S \sim 730\,^{\circ}\mathrm{C}$ for 13 min, the $4\times$ pattern appears in RHEED [Fig. 2(a)]. STM imaging of the $4\times$ surface reconstruction is presented in Fig. 2(b), during which the bias voltage polarity was flipped twice. Clearly, the $4\times$ surface consists of rows aligned along [110] with periodicity along $[1\bar{1}0]$ of $4a$.

Alternating the V_S between $+1.2$ and -1.2 V shows the registry between empty and filled states, which are evidently 180° out of phase, as seen in Fig. 2(c) showing the averaged line-profiles lpA, lpB, and lpC of areas A, B, and C, respectively. Such a phase shift is consistent with semiconducting surface states, in which the occupied and unoccupied wave functions are spatially separated [19].

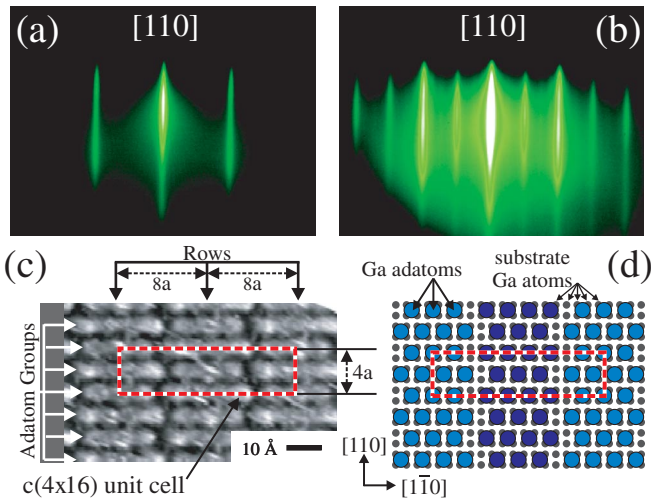

FIG. 1 (color). (a),(b) RHEED patterns of c-GaN(001) after growth under Ga-rich conditions; T_S during RHEED acquisition were 490 and 27 °C, respectively. (c) The STM image of the "2×" surface acquired at 27 °C, showing the $c(4 \times 16)$ reconstruction. $V_S = +0.5$ V; $I_T = 0.6$ nA. (d) A schematic model of the $c(4 \times 16)$ surface reconstruction.

To investigate the electronic structure of the $4\times$ surface, STS measurements were performed. Figure 3 shows, versus V_S, the tunneling current I_T and the derived normalized conductance (NC) $= (dI/dV)/(\overline{I/V})$, which is proportional to the density of states (DOS). To reduce noise inside the band gap due to divergence of NC at the band edges, we have used a broadening of 0.15 V. By extrapolating curves fitted to the conduction and valence band DOS to zero, the surface band gap is measured as 1.14 eV.

To compare the STM data with the theoretical model, we performed *ab initio* calculations of the electronic states and the STM images. We used the SIESTA method [20], based on density functional theory in the local density approximation. Separable, norm-conserving pseudopotentials of the Troullier-Martins type [21] were used to describe the effect of the core electrons. We included nonlinear core corrections and relativistic effects in the pseudopotential generation. For the Ga atom, the $3d$ electrons were included in the core. The pseudopotential core radii for Ga were 2.08, 2.3, and 3.3 bohr for the s, p, and d channels, respectively, and 1.37 bohr for the N s and p channels. The valence wave functions were expanded in a basis set of localized atomic orbitals. We used a double-ζ polarized (DZP) basis set for Ga and N atoms. For surface Ga atoms, we optimized the DZP basis set by varying the orbital confinement.

Our calculations were done in a 4×1 slab geometry, with 11 alternating Ga and N layers. The lower surface was terminated by pseudo-H atoms (artificial H atoms with ionic and electronic charge of $1.25e$), saturating the Ga dangling bonds, to simulate the presence of the bulk. A vacuum of 10 Å was inserted between periodically repeated slabs. A uniform grid with an equivalent plane-wave cutoff of 100 Ry was used to perform the numerical integrations in real space. Integrations over the first

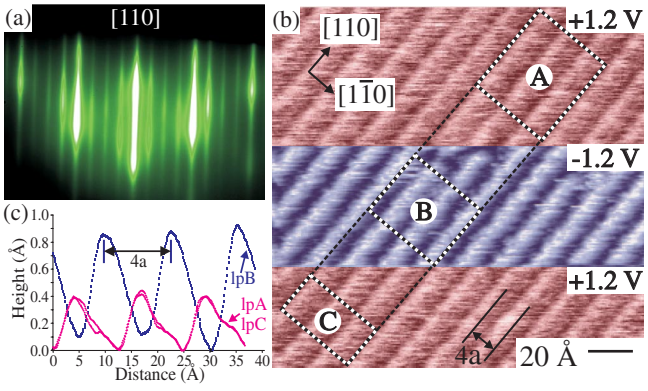

FIG. 2 (color). (a) RHEED pattern of c-GaN(001) after annealing at $T_S = 730\,^{\circ}\mathrm{C}$. (b) Dual-bias STM image on c-GaN(001); $I_t = 0.04$ nA. (c) Line profiles of the dual-bias image.

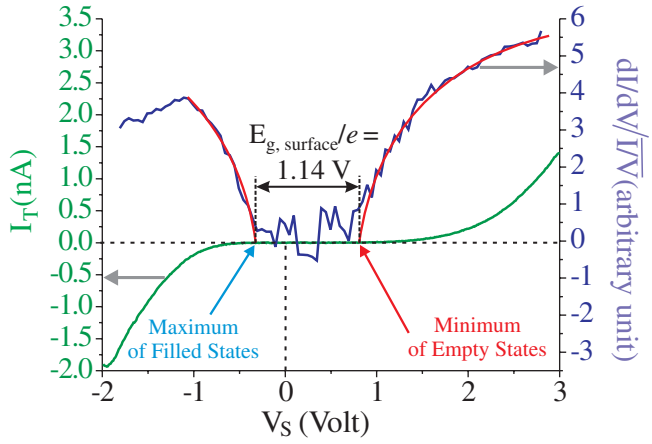

FIG. 3 (color). I_T vs V_S, averaged over 16 individual I-V spectra, acquired on the 4× surface reconstruction (left y axis), and normalized conductance vs V_S (right y axis). Red curves are fits to the conduction and valence band DOS. Peaks inside the band gap are noise.

Brillouin zone were replaced by discrete sums with a k-grid cutoff of 10 Å [22]. The system was relaxed using conjugate gradients.

The simulated surface reconstruction showed the formation of tetramer structures with distances of 2.68 Å between the two central Ga atoms and 2.66 Å between the central and end Ga atoms, slightly smaller than those obtained by Neugebauer *et al.* [15] using plane waves (2.73 and 2.71 Å, respectively). Furthermore, the calculated electronic band structure confirmed the existence of surface states in the gap as reported by Neugebauer *et al.* We obtained a surface band gap of 1.1 eV, similar to that found by Neugebauer *et al.* (1.2 eV) and this experiment (1.14 eV).

The 4×1 tetramer model consists of 4 Ga atoms joined together by 3 completely filled bonds. The end atoms each have one completely empty dangling bond. Thus, the peak of the filled-states STM corrugation should correspond to the center of the tetramer, and the peak of the empty states STM corrugation should correspond to the midpoint between tetramers.

Theoretical calculations of the electronic wave functions at the Γ point in the 4×1 tetramer model confirm the existence of three occupied and two unoccupied surface states. The occupied states have maxima at the positions of the internal bonds, while the unoccupied states have their minima there, with their maxima located at the position of the dangling bonds.

Figure 4 shows the 4×1 tetramer STM simulated images obtained using the Tersoff-Hamann approximation [23] as well as the simulated corrugation profiles, together with the experimental images. The simulations were obtained with a charge density of 1×10^{-4} $e/(\text{bohr})^3$ and convoluted with a Gaussian function (of 1.5 Å width) to take into account the finite resolution of the STM tip. Clearly, there is a good agreement between the STM images and the 4×1 tetramer model simulated images.

However, higher resolution STM images of this surface have been obtained, which the tetramer model cannot explain. As shown in the STM images of Figs. 5(a) and 5(d), periodicity is observed along [110]. For empty states ($V_S = +1$ V), this periodicity appears as evenly spaced depressions; for filled states ($V_S = -1$ V), it appears as a modulation of the row intensity. After precise image correction for thermal drift and x-y scanner asymmetry, the periodic structure of the images aligns perfectly with an ideal, rectangular 4×3 lattice. Also, shift boundaries between 4×3 domains occur, with shifts of $1/3$ of the $3\times$ spacing. The resultant incoherence is the likely explanation for why the $3\times$ was not previously seen in diffraction.

We furthermore observe that the empty states corrugation profile [Fig. 5(b)] shows a double peak structure, similar to that observed in the simulated profile [Fig. 4(f)]. A slight asymmetry is seen in the line profiles

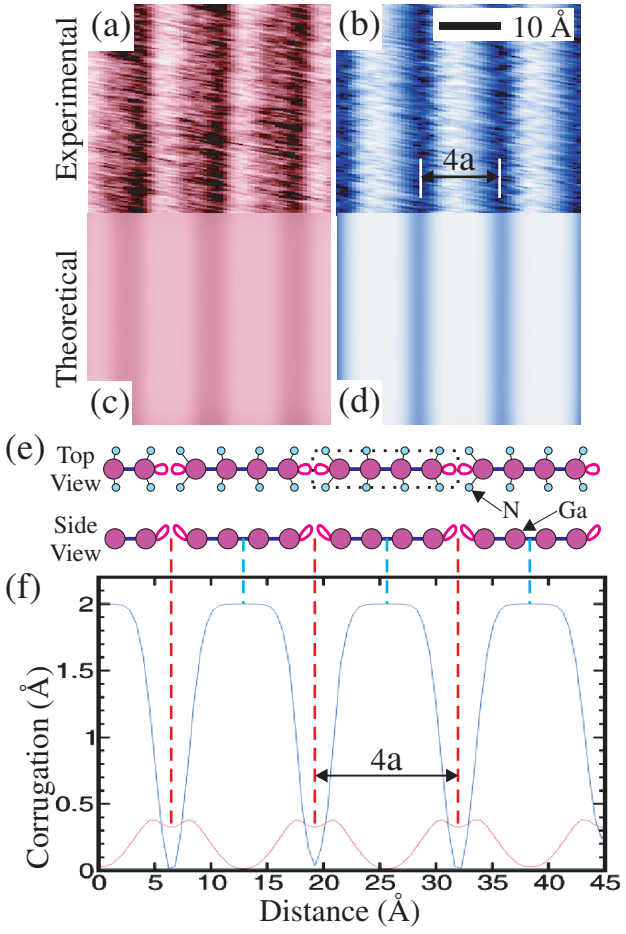

FIG. 4 (color). (a),(b) Experimental and (c),(d) simulated STM images for empty (red) and filled (blue) surface states. The simulated images correspond to isosurfaces of charge density equal to 1×10^{-4} $e/(\text{bohr})^3$ and convoluted with a Gaussian (of 1.5 Å width) to account for finite tip resolution; (e) 4×1 tetramer model with (f) simulated height profiles, corresponding to (c) and (d).

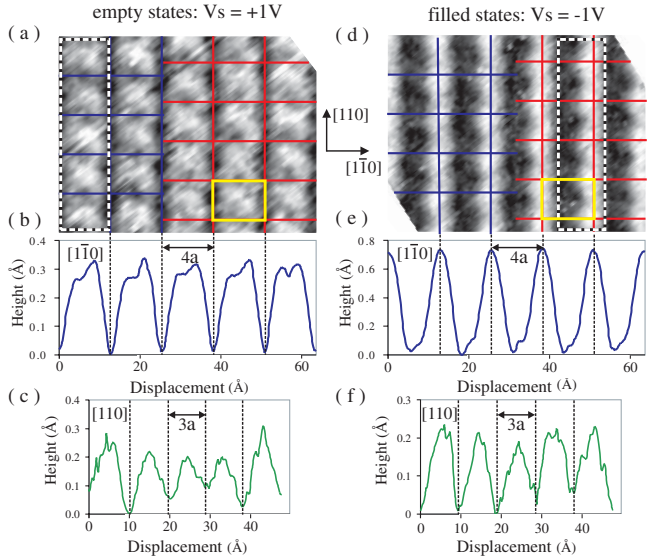

FIG. 5 (color). High-resolution STM images of 4×3 reconstruction. (a) Empty states image with corresponding average line profiles, (b) and (c), along $[1\bar{1}0]$ and [110], respectively. (d) Filled states image with corresponding average line profiles, (e) and (f), along $[1\bar{1}0]$ and [110], respectively. A shift boundary is evident from the blue and red overlaid 4×3 grids. Small yellow rectangles represent single 4×3 unit cells. The $[1\bar{1}0]$ profiles are from the whole image areas, while the [110] profiles are from the white-dashed box regions.

of Figs. 5(b) and 5(e) but is different from that seen in Fig. 2(c). As these images were taken under different tip conditions, these asymmetry effects are ascribed to tip asymmetry.

The 4×1 tetramer simulations predict a corrugation along [110] of $1\times$ (not seen here due to Gaussian convolution) rather than the observed $3 \times$. Clearly a new or modified model is needed. Possibilities include tetramer vacancy, octomer, or buckling models having a $3\times$ period along [110]. Note, however, calculations did not find buckling for the 4×1 tetramer model.

In conclusion, the clean *c*-GaN(001) surface structure has been investigated using a combination of STM and theory simulation. High-resolution STM images show that the intrinsic reconstruction is 4×3. Nonetheless, the 4×1 tetramer model successfully predicts the 180° phase shift between filled and empty states as well as a surface band gap consistent with the experiment. Thus, the tetramer model is a useful starting point, but future theory work is needed to determine a new model which can explain the $3\times$ periodicity. Whether or not that new model will consist of Ga tetramers remains to be seen.

We gratefully acknowledge M. Kordesch and H. Richardson for CL measurements helping to confirm the zinc-blende crystal structure. This material is based upon work supported by NSF under Grants No. 9983816 and No. 0304314. P. O. acknowledges Spain's MCyT Grant (No. BFM2003-03372-C03) and support for his visit to Ohio University from the PdMdI program of Spain's MEC.

[1] G. Binnig, H. Rohrer, Ch. Gerber, and E. Weibel, Surf. Sci. **131**, L379 (1983).
[2] R. M. Feenstra and J. A. Stroscio, J. Vac. Sci. Technol. B **5**, 923 (1987).
[3] T. Hasegawa, M. Nantoh, and K. Kitazawa, Jpn. J. Appl. Phys. **30**, L276 (1991).
[4] D. K. Biegelsen, R. D. Bringans, J. E. Northrup, and L. E. Swartz, Phys. Rev. B **41**, 5701 (1990).
[5] A. Kahn, Surf. Sci. **299–300**, 469 (1994).
[6] R. M. Tromp, R. J. Hamers, and J. E. Demuth, Phys. Rev. Lett. **55**, 1303 (1985).
[7] J. A. Kubby, J. E. Griffith, R. S. Becker, and J. S. Vickers, Phys. Rev. B **36**, 6079 (1987).
[8] M. D. Pashley, K. W. Haberern, W. Friday, J. M. Woodall, and P. D. Kirchner, Phys. Rev. Lett. **60**, 2176 (1988).
[9] C. D. MacPherson, R. A. Wolkow, C. E. J. Mitchell, and A. B. McLean, Phys. Rev. Lett. **77**, 691 (1996).
[10] A. R. Smith, R. M. Feenstra, D. W. Greve, J. Neugebauer, and J. E. Northrup, Phys. Rev. Lett. **79**, 3934 (1997).
[11] A. R. Smith, R. M. Feenstra, D. W. Greve, M.-S. Shin, M. Skowronski, J. Neugebauer, and J. E. Northrup, Surf. Sci. **423**, 70 (1999).
[12] O. Brandt, H. Yang, B. Jenichen, Y. Suzuki, L. Dáweritz, and K. H. Ploog, Phys. Rev. B **52**, R2253 (1995).
[13] M. Wassermeier, A. Yamada, H. Yang, O. Brandt, J. Behrend, and K. H. Ploog, Surf. Sci. **385**, 178 (1997).
[14] G. Feuillet, H. Hamaguchi, K. Ohta, P. Hacke, H. Okumura, and S. Yoshida, Appl. Phys. Lett. **70**, 1025 (1997).
[15] J. Neugebauer, T. Zywietz, M. Scheffler, J. E. Northrup, and C. G. Van de Walle, Phys. Rev. Lett. **80**, 3097 (1998).
[16] R. Miotto, G. P. Srivastava, and A. C. Ferraz, Physica (Amsterdam) **292B**, 97 (2000).
[17] T. Lei, T. D. Moustakas, R. J. Graham, Y. He, and S. J. Berkowitz, J. Appl. Phys. **71**, 4933 (1992).
[18] C. Constantin, M. Haider, H. A. H. AL-Brithen, R. Yang, E. Lu, and A. R. Smith (to be published).
[19] R. M. Feenstra, J. A. Stroscio, J. Tersoff, and A. P. Fein, Phys. Rev. Lett. **58**, 1192 (1987).
[20] J. M. Soler, E. G. Artacho, D. Julian, A. García, J. Junquera, P. Ordejón, and D. Sánchez-Portal, J. Phys. Condens. Matter **14**, 2745 (2002).
[21] N. Troullier and J. L. Martins, Phys. Rev. B **43**, 1993 (1991).
[22] J. Moreno and J. M. Soler, Phys. Rev. B **45**, 13 891 (1992).
[23] J. Tersoff and D. R. Hamann, Phys. Rev. Lett. **50**, 1998 (1983).